AIAA JOURNAL
Vol. 32, No. 11, November 1994

Shear and Compression Buckling Analysis for Anisotropic Panels with Elliptical Cutouts

V. O. Britt*
NASA Langley Research Center, Hampton, Virginia 23681

An approximate analysis for buckling of biaxial- and shear-loaded anisotropic panels with centrally located elliptical cutouts is presented. The analysis is composed of two parts: a prebuckling analysis and a buckling analysis. The prebuckling solution is determined using Lekhnitskii's complex variable equations of plane elastostatics combined with a Laurent series approximation and a boundary collocation method. The buckling solution is obtained using the principle of minimum potential energy. A byproduct of the minimum potential energy equation is an integral equation that is solved using Gaussian quadrature. Comparisons with documented experimental results and finite element analyses indicate that the approximate analysis accurately predicts the buckling loads of square biaxial- and shear-loaded panels having elliptical cutouts with major axes up to 60% of the panel width. Results of a parametric study are presented for shear- and compression-loaded rectangular anisotropic panels with elliptical cutouts. The effects of panel aspect ratio, cutout shape, cutout size, cutout orientation, laminate anisotropy, and combined loading on the buckling load are examined.

Nomenclature

A = ellipse minor axis
B_{kn} = constant coefficients of Laurent series
C_{mkn} = coefficients of Laurent series constants
D = circular cutout diameter and ellipse major axis
D_{ij} = bending stiffness constants
E_x = average elastic modulus in x direction
E_y = average elastic modulus in y direction
F = Airy stress function
F_m = applied force resultants at panel boundaries
G_{xy} = average shear modulus
K = buckling coefficient
L = panel length
S = arc length on interior or exterior boundary
W = panel width
W_{mn} = out-of-plane displacement function constant
w = out-of-plane displacement
X_n = x component of boundary traction
Y_n = y component of boundary traction
z_k = complex variable defined as $z_k = x + \mu_k y$
ε_x = average strain in x direction
$\eta_{xy,x}$ = coefficient of mutual influence of the second kind that characterizes shearing in the x-y plane caused by a normal stress in the x direction
$\eta_{xy,y}$ = coefficient of mutual influence of the second kind that characterizes shearing in the x-y plane caused by a normal stress in the y direction
θ = fiber orientation angle
λ = loading parameter
μ_k = complex roots of the characteristic equation
ν_{xy} = Poisson's ratio
Π = total potential energy
ξ_i = transformation variable
σ_x = normal stress in the x direction
σ_y = normal stress in the y direction
σ_{xy} = shear stress
Φ_k = first derivative of ϕ_k
ϕ_k = functions of z_k that make up the stress function
Ψ = inclination angle of elliptical cutout
$\bar{()}$ = complex conjugate

Presented as Paper 93-1565 at the AIAA/ASME/ASCE/AHS/ASC 34th Structures, Structural Dynamics, and Materials Conference, La Jolla, CA, April 19–22, 1993; received June 21, 1993; revision received March 21, 1994; accepted for publication April 8, 1994.

*Aerospace Engineer, Aircraft Structures Branch, Structural Mechanics Division. Member AIAA.

Introduction

FLAT rectangular panels with cutouts are found in several aircraft structural components such as wing ribs and spars. Often, cutouts are necessary in these panels to form ports for access, inspection, electrical lines, and fuel lines or to reduce the overall weight of the aircraft. Because of their light weight and tailorability, composite materials are becoming increasingly more popular for the manufacturing of these panels. During flight, these panels experience a combination of loading conditions. Therefore, the stability of composite rectangular panels with cutouts under biaxial and shear loading conditions is an important factor in future aircraft design.

The majority of investigations on the stability of composite panels with cutouts have been conducted using finite element methods. Lin and Kuo[1] analyzed rectangular composite laminates with circular cutouts using a nine-node Lagrangian finite element technique. The mathematical formulation was based on a first-order shear deformation theory and the variational energy method. The critical buckling loads were determined for laminates that were subjected to uniaxial and biaxial loading. Vellaichamy et al.[2] used the general purpose finite element code ELFINI[3] to conduct an optimization study of square composite panels having elliptical cutouts and subjected to uniaxial, biaxial, and shear loading. The study concentrated on the effect on the buckling load of the cutout aspect ratio and cutout orientation with respect to the lateral axis. Finite element methods such as these produce accurate results; however, they are costly methods of performing parametric or design studies where various materials and geometries must be considered.

Classical analysis methods have also been developed to efficiently analyze the buckling behavior of composite panels with cutouts. Nemeth[4] approached the problem of compressive buckling of composite panels with square or circular cutouts by approximating the in-plane and out-of-plane displacements with truncated kinematically admissible series. The principle of minimum potential energy was used to solve for the prebuckling stresses, and the Trefftz criterion along with the principle of minimum potential energy was used to find the stability equations that could be solved for the buckling loads. Owen[5] used an analysis based on Lekhnitskii's[6] complex variable equations, boundary collocation, and a Laurent series approximation to solve for the prebuckling stresses and the principle

of minimum potential energy to determine the buckling loads of simply supported, shear-loaded panels with circular cutouts. Jones and Klang[7] used this method to study the combined shear and compression loading of rectangular panels with circular cutouts and expanded the method to include elastic boundary conditions.

The objective of the present paper is to extend the original work done by Owen to analyze the shear and compression loading of rectangular composite laminates with centrally located elliptical cutouts that may be oriented at a given angle to the lateral axis of the panel. The results of a parametric study are presented that indicate the effects of panel aspect ratio, laminate anisotropy, cutout size, cutout shape, cutout orientation, and combined loading on the shear and compression buckling loads of a panel. For the analysis, the prebuckling stresses are determined by substituting a truncated Laurent series into Lekhnitskii's complex variable equations for stresses, forces, and displacements. Using boundary collocation and a Laurent series approximation along with a least-squares approach, the force and displacement equations are satisfied at a discrete number of points along the panel boundaries to determine the stresses in the panel. For the buckling analysis, the approach of Nemeth is followed. The out-of-plane displacements are approximated by truncated kinematically admissible series that are selected to satisfy the boundary conditions. The results from the prebuckling analysis are used with the principle of minimum potential energy to obtain the buckling loads. The large matrix equation that results from the minimum potential energy equation is solved numerically using Gaussian quadrature.

Analysis

The objective of this analysis is to determine the buckling load of a finite anisotropic panel with a centrally located elliptical cutout. The configuration analyzed is shown in Fig. 1. The panel is of length L (in x direction) and of width W. The panel has either an elliptical or a circular cutout at its center. The circular cutout is of diameter D, and the elliptical cutout has a major axis D and a minor axis A. The major axis of the ellipse may be inclined at some angle Ψ to the y axis. The panel is subjected to a uniform applied axial compression stress σ_x and/or a uniform applied shear stress σ_{xy}. Displacement boundary conditions may also be imposed, but they are only used for comparison with experiment in this paper. The edges of the cutout are assumed to be traction free. The edges of the panel may be simply supported or clamped, as long as opposite edges have the same boundary conditions. The lamina fiber angles θ are measured with respect to the x axis. The analysis of this model consists of two parts: a prebuckling analysis and a buckling analysis.

Prebuckling Analysis

The prebuckling stress analysis is based on Lekhnitskii's complex variable equations.[6] This method assumes that the panel is in a state of plane stress and is loaded by in-plane forces that do not vary through the thickness. Thus, average material properties are employed in the present stress analysis. Detailed descriptions of this analysis are presented in Refs. 5 and 8. Stress analysis results are presented for rectangular shear- and compression-loaded anisotropic panels with elliptical cutouts in Ref. 8. A summary of the present stress analysis follows.

The biharmonic equation for an anisotropic material in terms of an Airy stress function F and the average material properties is

$$\frac{\partial^4 F}{\partial y^4} - 2\eta_{xy,x}\frac{\partial^4 F}{\partial y^3 \partial x} - \left(2\nu_{xy} - \frac{E_x}{G_{xy}}\right)\frac{\partial^4 F}{\partial y^2 \partial x^2} - 2\eta_{xy,y}\frac{E_x}{E_y}\frac{\partial^4 F}{\partial y \partial x^3} + \frac{E_x}{E_y}\frac{\partial^4 F}{\partial x^4} = 0 \tag{1}$$

This biharmonic equation can be simplified using the transformation

$$z_1 = x + \mu_1 y \qquad z_2 = x + \mu_2 y \tag{2}$$

where μ_1, μ_2, and their complex conjugates are the roots of the characteristic equation

$$\mu^4 - 2\eta_{xy,x}\mu^3 + \left(\frac{E_x}{G_{xy}} - 2\nu_{xy}\right)\mu^2 - 2\eta_{xy,y}\frac{E_x}{E_y}\mu + \frac{E_x}{E_y} = 0 \tag{3}$$

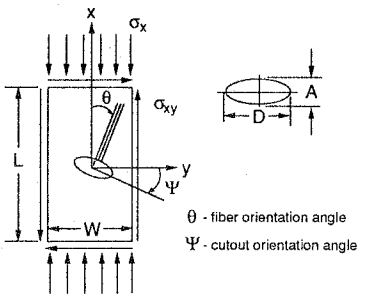

Fig. 1 Panel geometry and loading.

Using the transformation in Eq. (2), the generalized biharmonic equation can be written as

$$\frac{\partial}{\partial z_1}\frac{\partial}{\partial z_2}\frac{\partial}{\partial \bar{z}_1}\frac{\partial}{\partial \bar{z}_2}F = 0 \tag{4}$$

The solution for the stress function F is in the form

$$F = \phi_1(z_1) + \phi_2(z_2) + \overline{\phi_1(z_1)} + \overline{\phi_2(z_2)} \tag{5}$$

Applied displacements or tractions along the panel boundary can be related to the complex-valued stress function. The boundary tractions in the x direction, X_n, and in the y direction, Y_n, are related to the stress function by

$$\begin{aligned} 2\mathrm{Re}[\Phi_1(z_1) + \Phi_2(z_2)]|_{z_0}^{z} &= \pm\left(-\int_0^S Y_n\,\mathrm{d}S\right) \\ 2\mathrm{Re}[\mu_1\Phi_1(z_1) + \mu_2\Phi_2(z_2)]|_{z_0}^{z} &= \pm\int_0^S X_n\,\mathrm{d}S \end{aligned} \tag{6}$$

where S begins at a point z_0 and ends at z. The displacements are related to the stress fuction by

$$\begin{aligned} 2\mathrm{Re}[p_1\Phi_1(z_1) + p_2\Phi_2(z_2)] &= u \\ 2\mathrm{Re}[q_1\Phi_1(z_1) + q_2\Phi_2(z_2)] &= v \end{aligned} \tag{7}$$

and p_k and q_k are defined as

$$\begin{aligned} p_k &= \frac{1}{E_x}\mu_k^2 - \frac{\eta_{xy,x}}{E_x}\mu_k - \frac{\nu_{xy}}{E_x} \\ q_k &= \frac{\nu_{xy}}{E_x}\mu_k - \frac{\eta_{xy,y}}{E_y} - \frac{1}{E_y}\frac{1}{\mu_k} \end{aligned} \tag{8}$$

The complex-valued stress function $\Phi_k(z_k)$ is defined as

$$\Phi_k(z_k) = \frac{\partial \phi_k}{\partial z_k} \tag{9}$$

If the value of this stress function is known for every point within the panel boundaries, the stress distribution in the panel can be determined. In the present analysis, this stress function is represented by a truncated Laurent series containing unknown constant coefficients

$$\Phi_k(z_k) = \sum_{-N}^{N} B_{kn} z_k^n \tag{10}$$

The resultant force on every arc of the interior and exterior boundaries is known, and therefore Lekhnitskii's force equations can be used to solve for the unknown coefficients through boundary collocation. Satisfying the force loading conditions along the interior and exterior panel boundaries results in the following system of equations that can be solved for the unknown Laurent series constants:

$$[C_{mkn}]\{B_{kn}\} = \{F_m\} \tag{11}$$

A detailed discussion on determining the coefficients C_{mkn} is found on pp. 18–21 of Ref. 5. To improve solution convergence without increasing computation time, a least-squares approach is implemented. The least-squares method allows for an increase in the

number of force equations considered without an increase in the number of terms in the Laurent series. In the present analysis, twice as many equations as unknowns are considered; therefore, $[C_{mkn}]$ is a 16-row × 8-column matrix, $\{B_{kn}\}$ is an 8-row vector, and $\{F_m\}$ is a 16-row vector. To solve the system of equations for the unknown Laurent series coefficients, each side of the matrix equation is multiplied by the transpose of $[C_{mkn}]$. To improve the conditioning of the system matrix, the following mapping function that maps all of the points inside the panel boundaries to the exterior of a unit circle is used:

$$\xi_i = \frac{1}{A - i\mu_i D}\left(z_i + \sqrt{z_i^2 - A^2 - \mu_i^2 D^2}\right) \qquad i = 1, 2 \quad (12)$$

(See Fig. 1.) The use of this mapping function eliminates the problem of small numbers being raised to high powers. After the system of linear algebraic equations is solved for the Laurent series constants, the average in-plane stresses in the panel can be calculated using the following stress equations:

$$\sigma_x = \frac{\partial^2 F}{\partial y^2} = 2\mathrm{Re}\left[\mu_1^2 \Phi_1'(z_1) + \mu_2^2 \Phi_2'(z_2)\right]$$

$$\sigma_y = \frac{\partial^2 F}{\partial x^2} = 2\mathrm{Re}[\Phi_1'(z_1) + \Phi_2'(z_2)] \quad (13)$$

$$\sigma_{xy} = -\frac{\partial^2 F}{\partial x \partial y} = -2\mathrm{Re}[\mu_1 \Phi_1'(z_1) + \mu_2 \Phi_2'(z_2)]$$

where derivatives are taken with respect to z_i.

Buckling Analysis

Results obtained from the prebuckling analysis are used to determine the buckling load of the panel. The prebuckling stress distribution obtained from Eqs. (13) is substituted into the following equation representing the first variation of the second variation of the total potential energy Π. This is known as the Trefftz criterion for neutral equilibrium,

$$\delta[\delta^2 \Pi] = 0 \quad (14)$$

In Ref. 5 the expanded form of this stability equation for symmetrically laminated plates is given as

$$\int\int_A \left[D_{11} \frac{\partial^2 w}{\partial x^2} \delta \frac{\partial^2 w}{\partial x^2} + 2D_{16}\left(\frac{\partial^2 w}{\partial x \partial y} \delta \frac{\partial^2 w}{\partial x^2} + \frac{\partial^2 w}{\partial x^2} \delta \frac{\partial^2 w}{\partial x \partial y} \right) \right.$$

$$+ D_{12}\left(\frac{\partial^2 w}{\partial x^2} \delta \frac{\partial^2 w}{\partial y^2} + \frac{\partial^2 w}{\partial y^2} \delta \frac{\partial^2 w}{\partial x^2} \right)$$

$$+ 2D_{26}\left(\frac{\partial^2 w}{\partial y^2} \delta \frac{\partial^2 w}{\partial x \partial y} + \frac{\partial^2 w}{\partial x \partial y} \delta \frac{\partial^2 w}{\partial y^2} \right) + D_{22} \frac{\partial^2 w}{\partial y^2} \delta \frac{\partial^2 w}{\partial y^2}$$

$$+ 4D_{66} \frac{\partial^2 w}{\partial x \partial y} \delta \frac{\partial^2 w}{\partial x \partial y} - \lambda \sigma_x^0 \frac{\partial w}{\partial x} \delta \frac{\partial w}{\partial x} - \lambda \sigma_x^0 \frac{\partial w}{\partial y} \delta \frac{\partial w}{\partial y}$$

$$\left. - \lambda \sigma_{xy}^0 \left(\frac{\partial w}{\partial x} \delta \frac{\partial w}{\partial y} + \frac{\partial w}{\partial y} \delta \frac{\partial w}{\partial x} \right) \right] dA = 0 \quad (15)$$

where σ_x^0, σ_y^0, and σ_{xy}^0 are the prebuckling stresses in the panel. The out-of-plane deflection will be assumed to be a truncated kinematically admissible series that approximates the buckle mode of the panel and will take the following form:

$$w(x, y) = \sum_{m=1}^{N} \sum_{n=1}^{N} W_{mn} f_m(x) g_n(y) \quad (16)$$

For a simply supported panel, the deflection function is chosen to be

$$w(x, y) = \sum_{m=1}^{N} \sum_{n=1}^{N} W_{mn} \sin \frac{m\pi x}{L} \sin \frac{n\pi y}{W} \quad (17)$$

and for a clamped panel the deflection function is chosen to be

$$w(x, y) = \sum_{m=1}^{N} \sum_{n=1}^{N} W_{mn} \left[\cos \frac{(m-1)\pi x}{L} - \cos \frac{(m+1)\pi x}{L} \right]$$

$$\times \left[\cos \frac{(n-1)\pi y}{W} - \cos \frac{(n+1)\pi y}{W} \right] \quad (18)$$

Integration of the stability equation to obtain a closed-form solution is not feasible. The prebuckling stresses are functions in a complex domain, and conversion of the stresses from a complex domain to a real domain would be necessary for closed-form integration of the stability equation. Therefore, Gaussian quadrature is used to integrate the stability equations. The resulting system of equations constitutes an eigenvalue problem that can be solved to obtain the critical buckling load for the panel. A detailed description of the eigenvalue problem formulation is presented in Ref. 5.

Results and Discussion

Comparison with Experiment

A comparison between the current analysis and the experimental results found in Ref. 9 is shown in Fig. 2. The results are for a square, compression-loaded aluminum panel with a centrally located elliptical cutout. The compression load is applied by uniform edge displacements. The loaded edges of the panel are clamped, and the unloaded edges of the panel are simply supported. The panel size and the width of the elliptical cutout are held constant, and the elliptical-cutout-height-to-panel-width ratio A/W is varied from 0.1 to 0.7. The buckling load is plotted as a function of A/W, the cutout-height-to-panel-width ratio, in Fig. 2. The experimental results are denoted by the triangular symbols, and the analytical results are represented by the dashed line. The experimental and analytical results agree well except for A/W equal to 0.3. In Ref. 9 Nemeth notes that for this value of A/W the buckling mode shape consisted of an off-centered pattern. The presence of this nonsymmetric buckle pattern suggests that the introduction of the load into the panel was nonuniform due to improper machining of the loaded edges.

Comparison with Finite Element Analysis

Limited experimental buckling data exist for panels with circular and elliptical cutouts and subjected to shear loading or combined shear and compression loading. Thus, to verify the present analysis for shear and combined loading conditions, a finite element analysis was conducted using the STAGS[10] finite element computer program. A comparison of results obtained from this code and results from the present analysis is shown in Fig. 3. The results are for square simply supported laminated composite panels with centrally located circular cutouts. The panels are subjected to combined compression and shear loading. The compression loading is equal in magnitude to the shear loading. The lamina properties are listed in Table 1, and the laminates examined are $[(\pm 30)_6]_s$, $[(\pm 45)_6]_s$, $[(\pm 60)_6]_s$, and $[(\pm 45/0/90)_3]_s$. The buckling load is plotted as a function of cutout-diameter-to-panel-width ratio D/W, which is varied from 0

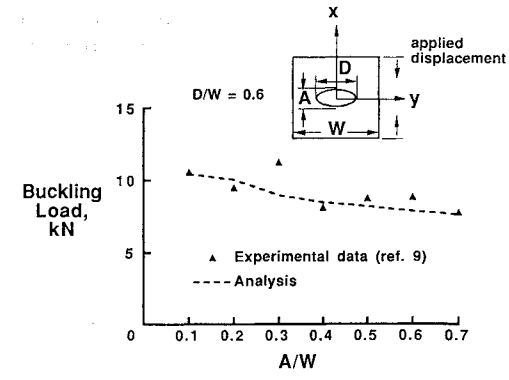

Fig. 2 Buckling loads for compression-loaded square aluminum panels with elliptical cutouts.

Table 1 Lamina properties of AS4/3502 graphite-epoxy material

Longitudinal Young's modulus, psi	18.5×10^6
Transverse Young's modulus, psi	1.6×10^6
Shear modulus, psi	0.832×10^6
Major Poisson's ratio	0.35

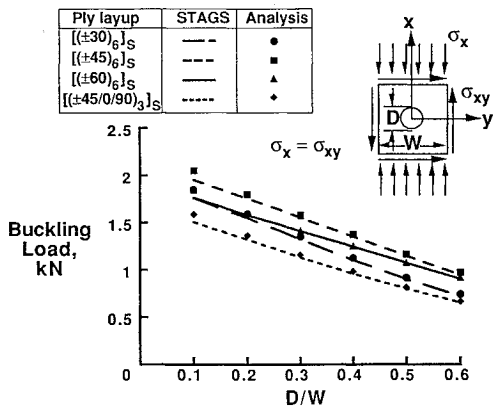

Fig. 3 Buckling loads for square shear- and compression-loaded composite panels with circular cutouts.

to 0.6. The finite element results are represented by lines, and results from the present analysis are denoted by symbols. For all cases, the finite element results agree well with the results from the present analysis.

Analytical Study

A study has been conducted for a range of parameters using the present analysis. The parameters considered are panel aspect ratio, laminate anisotropy, boundary conditions, cutout shape, and cutout orientation. All panels are stress loaded, and the results are presented in terms of a critical buckling stress σ_{cr} or a critical buckling coefficient K where

$$K = \frac{\sigma_{cr} W^2}{\pi^2 \sqrt{D_{11} D_{22}}} \tag{19}$$

where D_{11} and D_{22} are the laminate bending stiffnesses. The properties of all laminates analyzed are the same as AS4/3502 graphite-epoxy unidirectional tape, and the lamina properties are listed in Table 1. A Fortran program was written to implement the present analysis. This program can run on any computer having double precision capability for real and complex numbers, including most personal computers. The run time is comparable to that of a finite element analysis. However, the input file necessary to run the program consists of 10 lines and therefore requires a minimum amount of user time for model creation compared with a finite element analysis. In addition, convergence studies are very simple.

Results for Rectangular Panels with Circular Cutouts

To examine the effects of panel aspect ratio on the buckling load of a panel subjected to compression, shear, and combined compression and shear loading, we obtained buckling results for laminated rectangular panels with circular cutouts. The results for compression-loaded panels are shown in Fig. 4. In this figure, the critical buckling coefficient K is plotted as a function of panel aspect ratio L/W. The panel aspect ratio is varied from 1.0 to 4.0, and the cutout-diameter-to-panel-width ratio D/W is held constant at 0.3. Results are shown for four laminates: $[(\pm 30)_6]_s$, $[(\pm 45)_6]_s$, $[(\pm 60)_6]_s$, and $[(\pm 45/0/90)_3]_s$. The compression load is applied in the x direction, and the panel boundary conditions are either simply supported on all four edges or clamped on all four edges. In all cases, the buckling coefficients for the clamped panels are higher than for the simply supported panels, and greater variations are seen in the buckling coefficient curves for lower aspect ratios than for higher aspect ratios. For all panel aspect ratios and both clamped and simple support

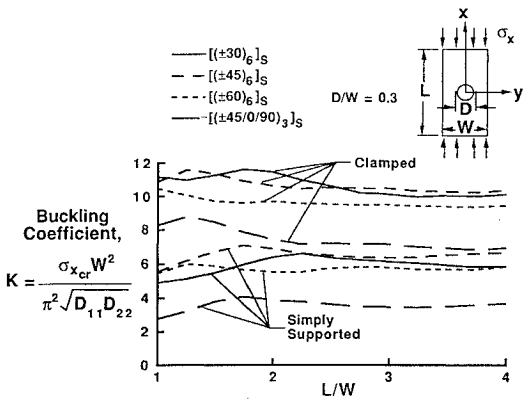

Fig. 4 Buckling coefficients for simply supported and clamped rectangular panels with circular cutouts and subject to compression loading.

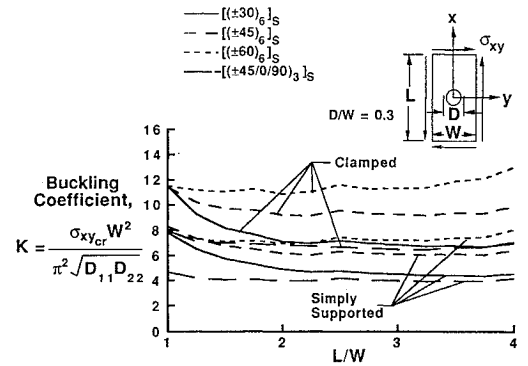

Fig. 5 Buckling coefficients for simply supported and clamped rectangular panels with circular cutouts and subject to shear loading.

boundary conditions, the $[(\pm 45)_6]_s$ laminates have higher buckling coefficients than the $[(\pm 60)_6]_s$ laminates, and the $[(\pm 60)_6]_s$ laminates have higher buckling coefficients than the $[(\pm 45/0/90)_3]_s$ laminates. For long panels, the $[(\pm 30)_6]_s$ laminates have buckling coefficients that are higher in value than the $[(\pm 60)_6]_s$ laminates but are lower in value than the $[(\pm 45)_6]_s$ laminates. However, for short panels, the relationship of the buckling coefficients for the $[(\pm 30)_6]_s$ laminates to the buckling coefficients for the $[(\pm 45)_6]_s$ and $[(\pm 60)_6]_s$ laminates varies with respect to the boundary conditions and panel length. For each laminate, the boundary conditions and the panel aspect ratio influence the buckling mode shape of the panel. These changes in mode shape contribute to the trends observed in the buckling coefficient curves.

Results for the rectangular panels subjected to an applied shear stress are shown in Fig. 5. Again, the clamped panels have higher buckling coefficients than the simply supported panels, but the buckling coefficient curves follow the same trends for both clamped and simple support boundary conditions. For a panel aspect ratio of 1, the buckling coefficients for the angle-ply $\{[(\pm\theta)_6]_s\}$ laminates are very close in value. As the panel aspect ratio increases, the angle-ply laminates with θ equal to 60 have the highest buckling coefficients, and the angle-ply laminates with θ equal to 30 have the lowest buckling coefficients. The buckling coefficients for the quasi-isotropic $[(\pm 45/0/90)_3]_s$ laminates are lower than the buckling coefficients for the angle-ply laminates for all panel aspect ratios. The 0- and 90-deg fibers in the quasi-isotropic laminate decrease the shear strength, resulting in low buckling loads for this laminate. For all four laminates, changes in the buckling modes are indicated by the festoon nature of the buckling coefficient curves.

Similar trends are shown for the same panels subjected to combined shear and compression loading in Fig. 6. For the combined loading case, the compression loading and the shear loading are equal in magnitude. The addition of the compression load to the shear-loaded panel reduces the buckling coefficient of the panel approximately by a factor of 2. For the combined loading conditions, the buckling coefficients for the $[(\pm 45)_6]_s$ laminates are much closer

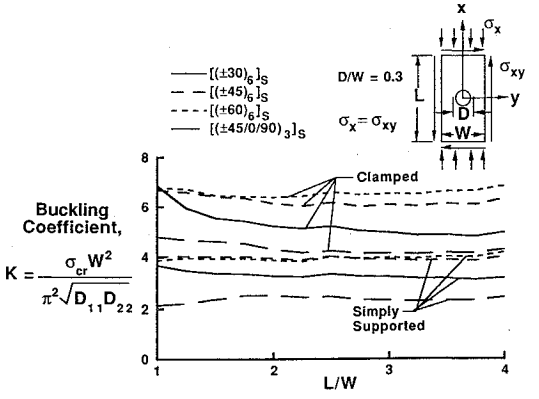

Fig. 6 Buckling coefficients for simply supported and clamped rectangular panels with circular cutouts and subject to shear and compression loading.

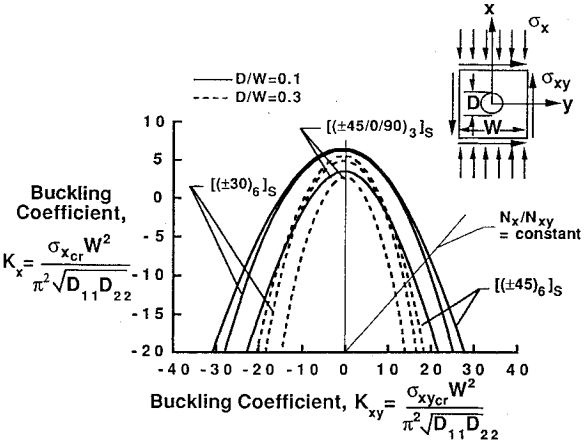

Fig. 7 Load interaction curve for a square simply supported panel with a circular cutout and subject to shear and compression loading.

in value to the buckling coefficients for the $[(\pm60)_6]_s$ laminates as compared with the buckling coefficients for these laminates in the case of shear loading only. For short panels with simple support boundary conditions, the $[(\pm45)_6]_s$ laminates have a slightly higher buckling coefficient than do the $[(\pm60)_6]_s$ laminates.

Results for Square Panels with Circular Cutouts Subjected to Combined Loading

To examine the effects of load interaction on panel buckling behavior, buckling coefficients are calculated for simply supported square panels with circular cutouts subjected to combined shear and axial compression or tension loading. The ratio of axial loading to shear loading is varied to exhibit the effects of an axial tension or compression load on the shear buckling behavior of a square panel. The axial buckling coefficient is plotted as a function of shear buckling coefficient in Fig. 7. The positive loading convention for the axial and shear stresses is indicated by the sketch on the figure. For example, negative values of the axial buckling coefficient correspond to a tension loading. The buckling coefficients are calculated for two cutout-diameter-to-panel-width ratios: $D/W = 0.1$, and 0.3. The solid lines correspond to $D/W = 0.1$ and the dashed lines correspond to $D/W = 0.3$. Three laminates are examined: $[(\pm30)_6]_s$, $[(\pm45)_6]_s$, and $[(\pm45/0/90)_3]_s$. A straight line emanating from the origin is shown on Fig. 7. Points of intersection between this straight line or any straight line emanating from the origin represent constant values of the loading ratio, N_x/N_{xy}. These lines are useful in examining the buckling resistance of different laminates to specific loading ratios.

The axis of symmetry of the load interaction curves is shifted slightly to the left of zero for all of the curves due to the bending anisotropy of the laminates. The quasi-isotropic $[(\pm45/0/90)_3]_s$ laminate experiences the least amount of shifting. Because of the laminate anisotropy, higher buckling loads result from application of

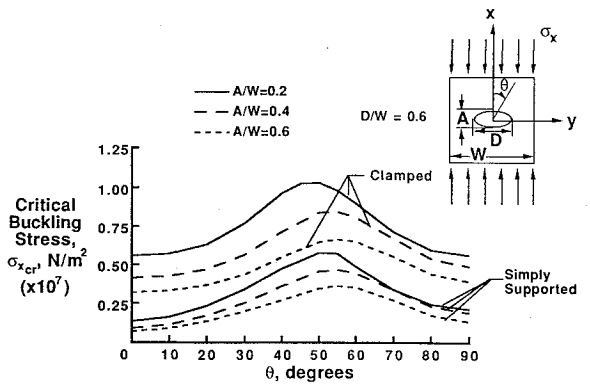

Fig. 8 Buckling loads for simply supported and clamped square $[(\pm\theta)_6]_s$ panels with circular cutouts and subject to compression loading.

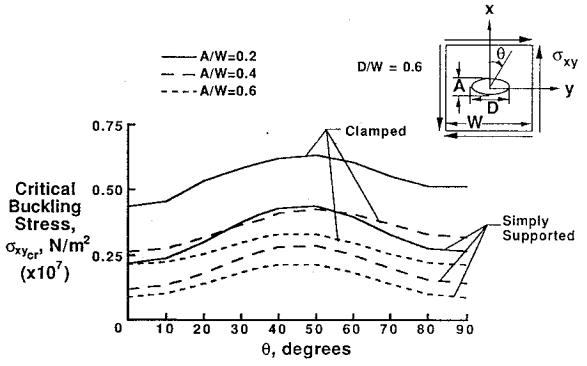

Fig. 9 Buckling loads for simply supported and clamped square $[(\pm\theta)_6]_s$ panels with circular cutouts and subject to shear loading.

negative shear loading than from positive shear loading given a constant applied axial compression or tension load. As noted previously for the rectangular laminates with circular cutouts, the angle-ply laminates have higher buckling coefficients than the quasi-isotropic laminates, and the $[(\pm45)_6]_s$ laminates have higher buckling coefficients than the $[(\pm30)_6]_s$ laminates.

Results for Square Angle-Ply Laminates with Elliptical Cutouts

Simply supported and clamped angle-ply laminates with elliptical cutouts are studied to determine the effects of ply orientation angle and elliptical cutout shape on buckling behavior. The critical buckling stress is plotted as a function of ply orientation angle θ for compression-loaded laminates in Fig. 8. The buckling stress has been chosen to be plotted instead of the buckling coefficient because the bending stiffnesses D_{11} and D_{22} change as a function of the ply orientation angle. The ply orientation angle ranges from 0 to 90 deg. For the cutout, the ellipse-major-axis-to-panel-width ratio D/W is held constant at 0.6. Three ellipse-minor-axis-to-panel-width ratios A/W are plotted, 0.2, 0.4, and 0.6, which are represented by the solid line, the long dashed line, and the short dashed line, respectively. The clamped laminates have higher critical buckling stresses than the simply supported laminates, but the trends for the critical buckling stress curves are similar for both boundary conditions. The critical buckling stress decreases as the cutout size increases, and the highest buckling stresses for a given cutout size occur at ply orientation angles between 45 and 55 deg. As the cutout size increases, the maximum buckling stress for a particular cutout size occurs at larger ply orientation angles. A discussion of compression-loaded square panels with circular cutouts found in Nemeth[11] suggests that, for certain ply orientations and cutout sizes, the axial prebuckling load path shifts away from the cutout. The result of this shift is an increase in the buckling load of the panel. The same result is observed for square panels with elliptical cutouts using the present analysis.

A plot for the angle-ply laminates subjected to an applied shear stress is shown in Fig. 9. Again, as cutout size increases, the buckling stress decreases. For a given cutout size, the clamped boundary

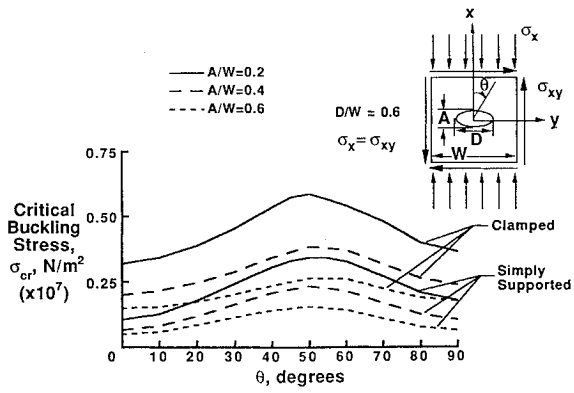

Fig. 10 Buckling loads for simply supported and clamped square $[(\pm\theta)_6]_s$ panels with circular cutouts and subject to shear and compression loading.

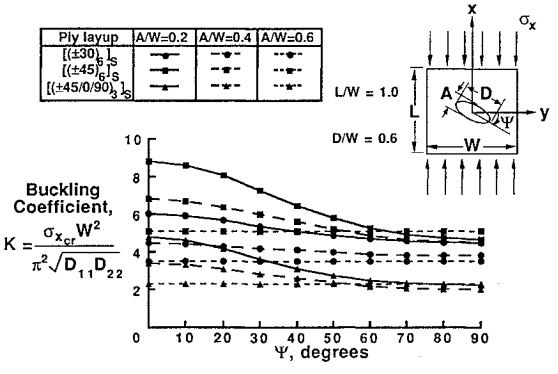

Fig. 11 Buckling coefficients for simply supported, compression-loaded square panels with elliptical cutouts oriented to the *y* axis.

condition provides a higher buckling stress than does the simple support boundary condition. For the circular cutout, $A/W = 0.6$, the maximum buckling stress occurs at a ply orientation angle of 45 deg, and the curve is symmetric about this angle. For the two elliptical cutouts, $A/W = 0.2$ and 0.4, the maximum buckling stresses occur at ply orientation angles of approximately 50 deg, and the curves are not symmetric.

A plot for the angle-ply laminates subjected to a combined shear and compression loading is shown in Fig. 10. For this case, the applied shear and compression stresses are equal in magnitude. The trends are similar to those seen in the plots for the compression- or shear-only load cases. The buckling stresses obtained for the panels loaded in shear only are approximately 7–21% higher than the buckling stresses for the combined load case. The buckling stresses obtained for panels loaded in compression only are 40–55% higher than the buckling stresses calculated for panels subjected to combined loading. The maximum buckling stresses occur at ply orientation angles between 50 and 60 deg for each cutout size.

Results for Square Laminates with Elliptical Cutouts Inclined to the y Axis

To examine the effects on the buckling behavior of cutout shape and cutout orientation with respect to the *y* axis, we calculated buckling stresses for square simply supported laminates with centrally located elliptical cutouts. Buckling coefficients for compression-loaded panels are plotted as a function of cutout orientation angle in Fig. 11. The cutout orientation angle Ψ ranges from 0 to 90 deg. (Note that, for cases involving shear loading, results for cutout orientation angles from 0 to −90 deg will be different than for orientation angles from 0 to 90 deg. Results for the negative angles will not be presented in this paper.) Results for $[(\pm 30)_6]_s$, $[(\pm 45)_6]_s$, and $[(\pm 45/0/90)_3]_s$ laminates are examined and are represented with circular, square, and triangular symbols, respectively. The elliptical cutout major-axis-to-panel-width ratio D/W is held constant at 0.6. The cutout minor-axis-to-panel-width ratio A/W is plotted for three values, 0.2, 0.4, and 0.6, which are represented by solid lines, long dashed lines, and short dashed lines, respectively. When $A/W = 0.6$, the cutout is circular, and therefore the buckling load

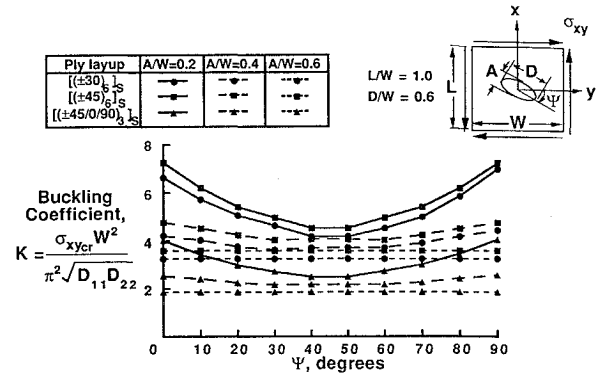

Fig. 12 Buckling coefficients for simply supported, shear-loaded square panels with elliptical cutouts oriented to the *y* axis.

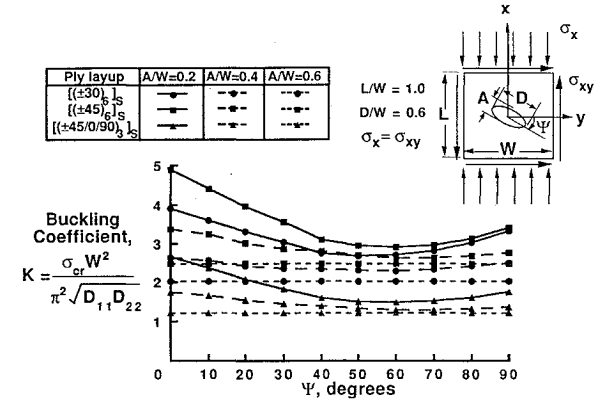

Fig. 13 Buckling coefficients for simply supported, shear- and compression-loaded square panels with elliptical cutouts oriented to the *y* axis.

remains constant with respect to the cutout orientation angle. For panels with the elliptical cutouts ($A/W = 0.2$ and 0.4), the highest buckling coefficients occur when the major axis of the elliptical cutout is aligned with the *y* axis ($\Psi = 0$ deg), and the lowest buckling coefficients occur when the major axis of the cutout is aligned with the *x* axis ($\Psi = 90$ deg). For all cutout orientation angles and elliptical cutout sizes, the $[(\pm 45)_6]_s$ laminate has the highest buckling coefficients and the $[(\pm 45/0/90)_3]_s$ laminate has the lowest buckling coefficients. For all cutout orientation angles for the $[(\pm 30)_6]_s$ laminate, the buckling coefficient remains constant or decreases as the cutout size increases. However, for the $[(\pm 45)_6]_s$ and $[(\pm 45/0/90)_3]_s$ laminates, this trend only occurs for cutout orientation angles of less than 50 deg. As the cutout orientation angles increase to values higher than 50 deg, panels with circular cutouts have higher buckling coefficients than panels with elliptical cutouts even though the elliptical cutouts are larger in area. This behavior suggests that the shifts in load path that accompany changes in the orientation angle of the elliptical cutout significantly affect the buckling load of the panel.

A plot for the $[(\pm 30)_6]_s$, $[(\pm 45)_6]_s$, and $[(\pm 45/0/90)_3]_s$ laminates subjected to an applied shear stress is shown in Fig. 12. The highest buckling coefficients occur when the elliptical cutouts are aligned with either the *y* axis or the *x* axis. The lowest bucking coefficients occur when the cutout is oriented at 45 deg to the *y* axis. For all cases, the curves are symmetric about the cutout orientation angle of 45 deg. For all laminates, the buckling coefficient decreases as the cutout size increases. As in the case of the compression-loaded panels, the $[(\pm 45)_6]_s$ laminate has the highest buckling coefficients, and the $[(\pm 45/0/90)_3]_s$ laminate has the lowest buckling coefficients.

A plot for the $[(\pm 30)_6]_s$, $[(\pm 45)_6]_s$, and $[(\pm 45/0/90)_3]_s$ laminates subjected to combined compression and shear stresses is shown in Fig. 13. The applied shear and compression stresses are equal in magnitude. As with the compression- or shear-only load cases, the highest buckling coefficients occur when the major axis of the elliptical cutout is aligned with the *y* axis. The lowest buck-

ling coefficients occur at a cutout orientation angle of 60 deg for all laminates and cutout sizes. As with the applied shear stress case, the buckling coefficients decrease as the cutout orientation angle increases for all laminates.

Concluding Remarks

A method for the buckling analysis of rectangular panels with elliptical cutouts and subjected to shear and/or axial compression or tension loading has been presented. The method consists of two parts: a prebuckling analysis based on Lekhnitskii's complex variable equations and boundary collocation and a buckling analysis based on the principle of minimum potential energy. The buckling loads are found for panels with circular and elliptical cutouts and subjected to compression, shear, and combined compression and shear loads. The effects of panel aspect ratio, laminate anisotropy, cutout size, cutout orientation, and load interaction on the buckling loads are examined. Results for $[(\pm 30)_6]_s$, $[(\pm 45)_6]_s$, $[(\pm 60)_6]_s$, and $[(\pm 45/0/90)_3]_s$ laminates are described to demonstrate the capabilities of the analytical method. To assess the accuracy of the method, analytical results are compared with experimental data for compression-loaded isotropic panels with elliptical cutouts. Results from the current analysis have also been compared with finite element analyses for anisotropic panels with circular cutouts and subjected to combined shear and compression loading. The results for the present analysis agree well with both the experimental data and the results obtained from finite element analysis.

To demonstrate the flexibility of the analytical method with respect to material properties, panel geometry, boundary conditions, and loading conditions, several laminates subjected to compression, shear, and combined loads have been analyzed. A study of simply supported and clamped rectangular anisotropic panels with circular cutouts has been conducted to assess the effects of panel aspect ratio on the panel buckling loads. The results indicate that the buckling curves experience greater variations with respect to the panel laminate for small panel aspect ratios and that the shear and compression buckling loads are reduced by approximately 50% when they are applied in combination and in equal magnitudes. To assess the buckling behavior of panels subjected to combined compression and shear loading where the ratio of shear to compression loading is varied, a study of simply supported square anisotropic panels with circular cutouts has been conducted. The results of this study indicate that the bending anisotropy of the panels results in slightly higher buckling loads from the application of negative shear than from the application of positive shear in the presence of a constant applied axial stress.

Results are also presented for anisotropic panels with elliptical cutouts and subjected to applied shear and/or axial compression loading to investigate the effects of ply orientation and cutout orientation on panel buckling behavior. A study of simply supported and clamped angle-ply laminates with elliptical cutouts aligned with the lateral axis has been conducted. This investigation shows that the ply orientation angle that gives the highest buckling loads is a function of cutout area as well as panel loading conditions. A study of simply supported, compression- and/or shear-loaded, square, anisotropic panels with elliptical cutouts oriented at a given angle to the lateral axis has been conducted to determine the effects of cutout orientation on the panel buckling behavior. This study indicates that, for compression loading, panels with elliptical cutouts oriented at certain angles to the lateral axis can have lower buckling loads than panels with circular cutouts, even though the circular cutouts are larger in area than the elliptical cutouts. For the panels loaded in shear and combined shear and compression, the buckling load decreases as cutout area increases for all cutout orientation angles.

The wide range of results obtained in the present study exemplifies the ability of the present method to adapt to many different panel sizes, cutout geometries, boundary, and loading conditions. The method allows for biaxial, shear, and combined loads as well as simple support and clamped boundary conditions. Although only traction loading conditions are considered in the present paper, the method is also capable of analyzing displacement loading conditions. The flexibility of this method illustrates its main advantage over the finite element method in the areas of structural design and optimization. Because the present method requires only 10 lines of input to describe the model, user modeling time is significantly less than for finite element analyses.

References

[1]Lin, C., and Kuo, C., "Buckling of Laminated Plates with Holes," *Journal of Composite Materials*, Vol. 23, June 1989, pp. 536–553.

[2]Vellaichamy, S., Prakash, B. G., and Brun, S., "Optimum Design of Cutouts in Laminated Composite Structures," *Computers and Structures*, Vol. 37, No. 3, 1990, pp. 241–246.

[3]Anon., "ELFINI Base Manual—General Introduction Manual," Avions Marcel Dassault-Breguet Aviation, France, 1988.

[4]Nemeth, M. P., "Buckling Behavior of Orthotropic Composite Plates with Centrally Located Cutouts," Ph.D. Dissertation, Virginia Polytechnic Inst. and State Univ., Blacksburg, VA, May 1983.

[5]Owen, V. L., "Shear Buckling of Anisotropic Plates with Centrally Located Circular Cutouts," M.S. Thesis, North Carolina State Univ., Raleigh, NC, May 1990.

[6]Lekhnitskii, S. G., *Anisotropic Plates*, Gordon & Breach, New York, 1968.

[7]Jones, K. M., and Klang, E. C., "Buckling Analysis of Fully Anisotropic Plates Containing Cutouts and Elastically Restrained Edges," AIAA Paper 92-2279, April 1992.

[8]Britt, V. O., "Analysis of Stresses in Finite Anisotropic Panels with Centrally Located Cutouts," DOT/FAA/CT-92-25-VOL-1, Nov. 1991, pp. 695–706.

[9]Nemeth, M. P., "Buckling and Postbuckling Behavior of Compression-Loaded Isotropic Plates with Cutouts," NASA TP 3024, Sept. 1990.

[10]Almroth, B. O., and Brogan, F. A., "The STAGS Computer Code," NASA CR-2950, Feb. 1978.

[11]Nemeth, M. P., "Buckling Behavior of Compression-Loaded Symmetrically-Laminated Angle-Ply Plates with Holes," *AIAA Journal*, Vol. 26, No. 3, 1988, pp. 330–336.